ACDIV-2013-13
September, 2013

FIRST TRANSVERSE BEAM SIZE MEASUREMENTS USING INTERFEROMETRY AT ALBA

U. Iriso, L. Torino, T. Mitsuhashi (KEK)

Abstract:

Double-slit interferometry using visible light has been used for measuring the transverse beam size in different accelerators. The beam size is inferred from the analysis of the spatial coherence of the synchrotron light produced by a bending magnet. At ALBA, this technique has been implemented with moderate success, mainly limited by the present imperfections in the in-vacuum mirror that is used to extract the light out of the vacuum chamber. In this paper, we report the results obtained with the current set-up, and discuss possible improvements.

FIRST TRANSVERSE BEAM SIZE MEASUREMENTS USING INTERFEROMETRY AT ALBA

U. Iriso, L. Torino, ALBA-CELLS, Cerdanyola, Spain
T. Mitsuhashi, KEK, Tsukuba, Japan

Abstract

Double-slit interferometry using visible light has been used for measuring the transverse beam size in different accelerators. The beam size is inferred from the analysis of the spatial coherence of the synchrotron light produced by a bending magnet. At ALBA, this technique has been implemented with moderate success, mainly limited by the present imperfections in the in-vacuum mirror that is used to extract the light out of the vacuum chamber. In this paper, we report the results obtained with the current set-up, and discuss possible improvements.

INTRODUCTION

Since the Storage Ring (SR) commissioning in 2011, ALBA is measuring the electron transverse beam size with the classical pinhole system using the x-ray part of the synchrotron radiation produced in dipole BM32 [1, 2]. In order to have further ways to measure the machine transverse emittance, we decided to develop a double-slit interferometry system using the visible part of the synchrotron radiation, as already performed in other machines [3, 4, 5].

In this case, we use the visible light coming from the radiation produced by the bending dipole BM01 that is currently arriving at the diagnostics beamline Xanadu, and that it is currently used to perform longitudinal studies using the streak camera [6]. Using a light splitter, we direct part of the light towards a double slit system to perform interferometer measurements. Since Xanadu was foreseen only for longitudinal studies, we will see that certain limitations arise when trying to measure the transverse beam sizes. Table 1 lists the main SR parameters and the theoretical beam sizes for both BM01 and BM32.

Table 1: ALBA SR Parameters and Expected Beam Sizes at Dipoles BM32 (Pinhole) and BM01 (Interferometry).

Parameter	BM01	BM32
hor beam size, σ_x [um]	54.2	57.2
ver beam size, σ_y [um]	23.8	28.3
hor emit., ϵ_x [nm-rad]	4.6	
coupling, %	0.5	
beam energy, E [GeV]	3.0	
bending radius, ρ [m]	7.05	

In this report, we describe the experimental set-up developed using the available instrumentation, show the first results obtained with it, and discuss the present limitations and future outlook of this project.

INTERFEROMETER SET-UP

The measurement principle is explained in detail in Refs. [3, 7]. In summary, it is based on the interferogram produced by monochromatic and polarized synchrotron light after passing through a double slit. When these two beamlets are focused into a CCD camera, the electron beam size can be inferred from the visibility of the interferogram, which indicates the complex degree of spatial coherence of the photons.

At the image plane, and considering that the two slits are illuminated with the same intensity, the light distribution is:

$$I(x) = I_0 \ \mathrm{sinc}^2\left(\frac{2\pi w}{\lambda d_1}x + \phi_s\right)\left[1 + V\cos\left(\frac{2\pi D}{\lambda d_1}x + \phi_c\right)\right] \ , \quad (1)$$

where λ is the light wavelength, w is the slit width, d_1 is the distance between the slits and the CCD, and D is the separation between slits. ϕ_s and ϕ_c are relative phases. The visibility V is related to the complex degree of coherence, and it is inferred as:

$$V = \frac{I_{\max} - I_{\min}}{I_{\max} + I_{\min}} \ , \quad (2)$$

where $I_{\max}$ and $I_{\min}$ are the maximum and minimum intensity at the interference fringe. For a point-like source, $V = 1$, but an extended source smears out the interference fringe. This allows the calculation of the beam size by:

$$\sigma = \frac{\lambda d_0}{\pi D}\sqrt{\frac{1}{2}\ln\left(\frac{1}{V}\right)} \ , \quad (3)$$

with d_0 the distance between the source point and the double slit system.

Figure 1 shows a sketch of the experimental setup. The synchrotron radiation is produced at dipole BM01, and the crotch absorbers limit the angular apertures to ±1.85 mrad (hor) and ±3.0 mrad (ver). Only the visible part is reflected using the in-vacuum half mirror, whose vertical position is remotely controlled. Even at its lowest vertical position (0.85 mrad), the mirror does not interfere with the x-rays, and it only reflects the visible light. The light travels then in atmospheric pressure and is guided to the optical hutch through a set of 6 conventional mirrors to the experimental hutch.

The double slit system is placed at the optical table, at a distance of 15 m from the source point (see Fig. 1). After

passing through a monochromator and a polarizer that selects between the horizontal and vertical polarization, the two light beamlets are focused onto the CCD camera using a refractive lens. An image of the spot size arriving at the optical table is shown in Fig. 2.

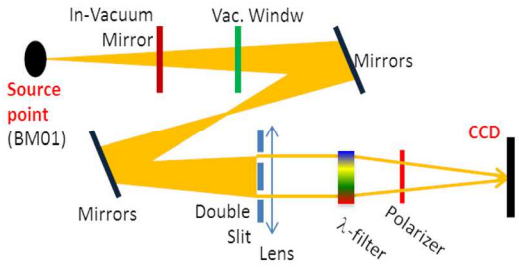

Figure 1: Layout of the interferometer setup. The radiation produced at the dipole BM01 is directed towards the optical table using one in-vacuum mirror and 6 in-air mirrors (plane and non-focusing). The distance from the source point to the double slit system is 15 m.

Wavefront Distortion

The synchrotron radiation interferometer is a wavefront division-type two-beam interferometer of polarized and (ideally) monochromatic light. For this reason, it is very important to keep an homogenous wavefront along the transport line. This includes the in-vacuum mirror, vacuum window, in-air mirrors, and other optomechanical components present in the light path – see Fig. 1.

However, we found that the wavefront arriving at the double slit system was not very homogenous, as shown in Fig. 2. The presence of the vertical and horizontal dark stripes indicate that the optical quality of the light path is non-appropriate, in particular, that the light is being reflected by a mirror with a non-appropriate surface flatness. Other effects that contribute to this image deterioration are the blackening and non-parallelism of the vacuum window, and dust at the in-air optical mirrors. Since this beamline was originally designed to measure the bunch length using a streak camera and not to implement interferometer measurements, detail attention was not taken to these parameters.

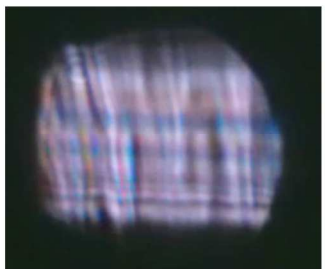

Figure 2: Picture of the light arriving at Xanadu optical hutch after all the M6 mirror. The dimensions are approximately 50x30mm.

This fact made very difficult to focus the system onto the CCD camera. The sequence shown in Fig. 3 describes the effect of trying to focus the image spot using a Hartmann mask located at the double-slit system. By displacing the focusing lens along the light path, we try to find the point where all the spots from the Harmann mask converge into one, but this could not clearly found. The best location is shown in Fig. 3, (bottom-left), and even there the zoom of the central region reveal the presence of 3 spots.

This points out that possible slope aberrations are present in the in-vacuum mirror, which is an expected effect after two years of operation. This is further proven by the image given by the Hartmann mask (see top-right plot at Fig. 3). While typically the required mirror surface flatness is $\lambda/8$ (peak-to-valley, ptv), currently this is $\sim \lambda/2$ (at best, according to the manufacturer of the in-vacuum mirror).

Presently, we are manufacturing a new mirror with a surface flatness of $\lambda/10$. This ptv value is also required for the new vacuum window, from which we also require a parallelism below 5 arcsec. A more quantitative evaluation of the in-vacuum mirror surface flatness using the Hartmann mask could not be done at the time of this test, but it is currently foreseen for the near future.

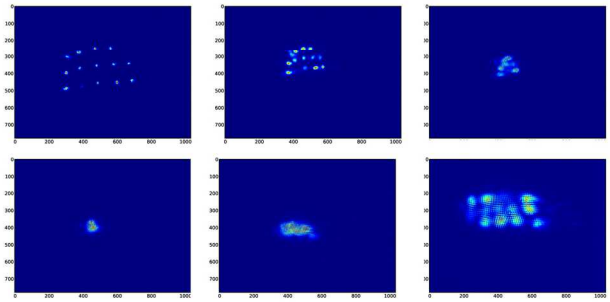

Figure 3: Focusing sequence of the Hartmann mask.

EXPERIMENTAL RESULTS

We perform transverse beam size interferometer measurements by carefully chosing the position of the slit with respect to the light wavefront. In most cases, the position of the two slit system sampling the light spot shown in Fig. 2 had an influence in the interferogram pattern and so the reproducibility was not straight forward. For this reason, we show first the estimation of the experimental error and next, we show the results in both horizontal and vertical plane for different slit separations.

Error Analysis

The beam size error with respect to the visibility fringes is analyzed in Refs. [7], showing that optimum visibility values shall be around 0.5. Here, we further show the beam size error with respect to CCD pixel intensity I, which is obtained from error propagation of Eqs. 2 and 3:

$$\frac{d\sigma}{\sigma} = \frac{2\,dI}{I_{\max}\,(1-u)\,\ln\frac{1+u}{1-u}}\,, \tag{4}$$

where $u = I_{\min}/I_{\max}$ is the ratio between the minimum and maximum of the interference fringe, and dI is the error of the CCD pixel intensity. This plot is depicted in Fig. 4 for a reasonable case where $dI/I_{\max}$ =1%. Our CCD camera is a Basler Scout of 14 bits resolution. Figure 4 shows that in order to have error bars below 10%, it is important to avoid the regions where $u \to 1$ (where $I_{\min}$ might be in the order of the light background noise), and $u \to 0$ (no interference fringe). We can also see that optimum values of the visibility are also around 0.5, while for $V \to 1$ the error bar increases significantly.

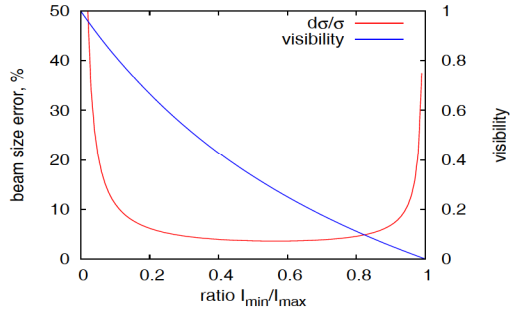

Figure 4: Visibility and beam size error wrt ratio between max and min of interference fringe when $dI/I_{\max} = 1\%$.

Horizontal Plane

An example of the interferogram obtained with the current setup is shown in Fig. 5. In order to minimize the effect of the wavefront distortion, the image analysis is only performed inside the white rectangle (our Region Of Interest, ROI). The horizontal projection of this ROI is depicted by a white trace inside Fig. 5, from where we obtain the intensities $I_{\max}$ and $I_{\min}$ of the interference fringes. From them, we compute V and thus the beam size σ_x.

We repeat the measurement for different slit separations. For each slit, we perfom 10 measurements. The average value for each slit are shown in Fig. 6: the solid line corresponds to the fit, which evaluates the degree of coherence of the results. The discrepancies between the results and the fit indicate that the degree of coherence of the wavefront is not very good, as shown in the previous section. Nevertheless, the values listed in Tab. 2 are in very good agreement with the expected values shown in Tab. 1 and the emittance values provided by the pinhole measurements at the same time.

Vertical Plane

Although in the vertical plane it was more difficult to find a region with an homogenous wavefront, the same scan was carried out. An example for the case of a slit separation D = 18 mm is shown in Fig. 7. As for the horizontal case, the image analysis is performed for the ROI marked with a white rectangle inside the image.

Figure 8 shows the visibility for the different slit separation. However, if we repeat the procedure as in the case

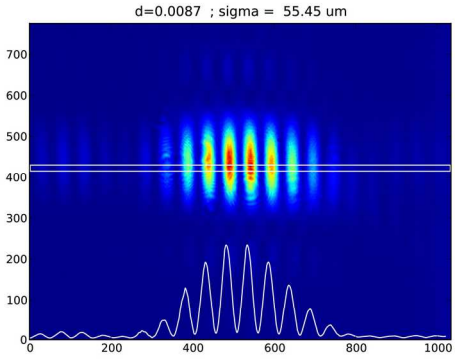

Figure 5: Example in the horizontal plane. The projection shown inside the image corresponds only to the ROI.

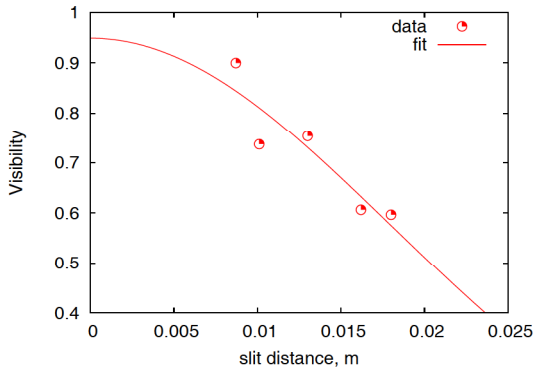

Figure 6: Horizontal visibility as a function of slit separation.

of the horizontal plane, in this case we found a vertical beam size $\sigma_y = 32\mu$m±15% (see Tab. 2), which is larger and not consistent with the theoretical values in Table 1. This is because the intensity arriving at each slit is not the same, and so we try to correct for this effect. This is similar to the procedure shown in [5], but in this case, the imbalance between slit 1 and 2 is not produced in purpose and in a controlled way, but produced by default due to the unhomogenous wavefront. Therefore, the visibility in Eq. 1 needs to consider the imbalance factor:

$$\nu = 2\frac{\sqrt{I_1 I_2}}{I_1 + I_2}\,, \tag{5}$$

where I_1 and I_2 are the light intensities illuminating slit 1 and 2, respectively. These are evaluated by completely covering one or the other and take the image provided by a each single separated slit.

Table 2 shows the results in all cases. Note that after correcting for the imbalance factor, still the vertical case shows a significant discrepancy with respect to the theoretical case, and only a good agreement is shown for the case D=18.0 mm (corresponding to the smallest visibility, and so the smallest error bar). Figure 8 shows the effect of correcting the effect of the imbalance factor. In this case,

the vertical beam size obtained by averaging all values is $\sigma_y = 29\ \mu$m $\pm 20\%$. The reason for the large fit error bar stems in the large values of the visibility, as shown in Fig. 4. In order to decrease V and so decrease the measurement error bar, larger slit separations are needed. But we are presently limited by the surface light footprint. For this reason, the new in-vacuum mirror is being designed with a larger reflecting surface, which will allow the use of slits with larger separation D.

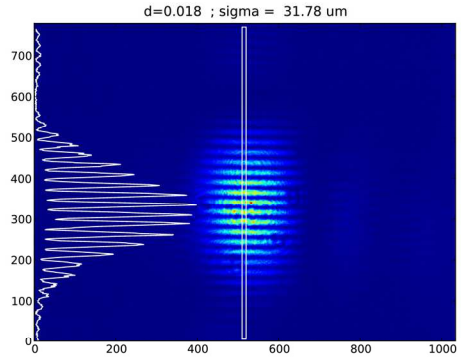

Figure 7: Example in the vertical plane. The projection shown inside the image corresponds only to the ROI (white rectangle inside the picture).

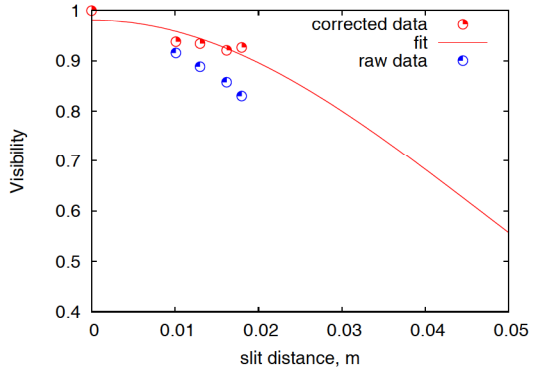

Figure 8: Vertical visibility as a function of slit separation for the raw data (blue points) and correcting for the imbalance effect (red).

CONCLUSIONS AND OUTLOOK

The results summary are listed in Tab. 2, for both horizontal and vertical cases, and in the latter case, it also includes the imbalance factor and the corrected σ_y. While in the horizontal case the results are not far from the expected values, in the vertical plane the results needed careful treatment due to the "default" in-balance effect. This is explained by the largest V values in the vertical plane (around 0.9), while for the horizontal case this value goes down to around 0.6. In all cases, the optimum results were only obtained after scanning the double slit system along the light wavefront and often the reproducibility was not straightforward.

Table 2: Results Summary Obtained for the Horizontal and Vertical Plane, for the Latter Case we also Consider the Effect of the Intensity Imbalance Factor ν.

D, mm	σ_x, μm	$\sigma_y^{\mathrm{raw}}, \mu$m	$\sigma_y^{\mathrm{corr}}, \mu$m
10.1	56.7	39.5	37.3
13.0	52.2	32.6	29.9
16.2	53.0	30.1	26.3
18.0	52.1	27.1	22.7
Average:	**53.6 ±3%**	**32.3 ±15%**	**29.0 ±20%**

Although the results are not far from the theoretical values (especially for the horizontal case), the system is still not ready to be used as a tool from on-line beam size monitoring. For this reason, several upgrades are foreseen. We are in the process of exchanging the in-vacuum mirror from a new one having a better ptv surface flatness (to keep the wavefront homogenous) and a larger reflecting surface in order to obtain lower visibility values, which have been especially a limiting factor in the vertical plane. Not only the in-vacuum mirror, due care will be taken to make sure that the rest of the components along the optical path do not deteriorate the light wavefront (vacuum window parallelism and surface flatness, optical mirrors, etc).

ACKNOWLEDGMENTS

We thank J. Ferrer by help on the slit preparation, G. Benedetti for the calculations with MML, and both CELLS and KEK to easily allow the collaboration between both labs.

REFERENCES

[1] U. Iriso, et al, *Diagnostics during the ALBA SR commissioning*, Proc. of DIPAC'11, Hamburg (Germany).

[2] U. Iriso, *Beam size and emittance measurements using the ALBA Pinhole*, AAD-SR-DI-PINH-01.

[3] T. Mitsuhashi, *Measurement of small transverse beam size using interferometry*, Proc. of DIPAC'2001, Grenoble (France).

[4] S.T. Wang et al, *Horizontal beam-size measurements at CESR-TA using synchrotron light interferometry*, MOPPR079, Proc. of IPAC'2012, New Orleans (USA).

[5] M.J. Boland (ALS), T. Mitsuhashi (KEK), K.P. Wootton (Univ. of Melbourne), *Intensity imbalance optical interferometer beam size monitor*, Proc. of IBIC'2012, Tsukuba (Japan).

[6] U. Iriso and F. Fernandez, *Streak Camera Measurements at ALBA: Bunch Length and Energy Matching*, Proc. of IBIC'2012, Tsukuba (Japan).

[7] T. Mitsuhashi, Proc. of the Joint US-CERN-Japan- Russia School, Montreux, May 1998, pp. 399-427.